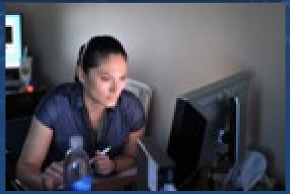

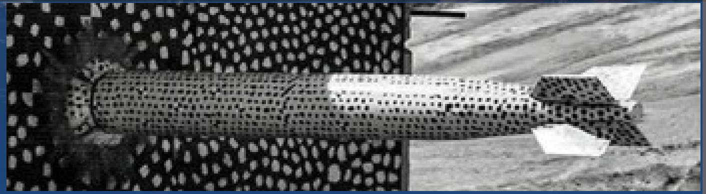

Coupling magnetic and mechanical phenomena with LAMMPS

PRESENTED BY

Julien Tranchida

Contact: jtranch@sandia.gov

A computational model coupling micro-structure and magnetic properties

Molecular dynamics

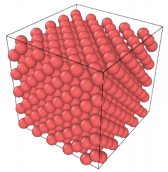

- Enables: defects, inhomogeneities, phase-transitions, ...
- Limitations: do not account for magnetization.

A computational model coupling micro-structure and magnetic properties

Molecular dynamics

- Enables: defects, inhomogeneities, phase-transitions, ...
- ✖ Limitations: do not account for magnetization.

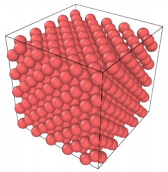

Spin dynamics

- Enables: magnetization dynamics, spin textures, ...
- ✖ Limitations: structural defects, fixed lattice.

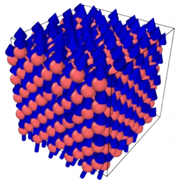

A computational model coupling micro-structure and magnetic properties

Molecular dynamics

- Enables: defects, inhomogeneities, phase-transitions, ...
- Limitations: do not account for magnetization.

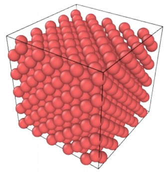

Spin dynamics

- Enables: magnetization dynamics, spin textures, ...
- Limitations: structural defects, fixed lattice.

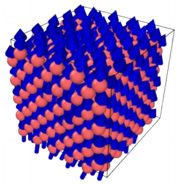

SPIN package, coupled SD - MD

$$
\begin{cases}
\dfrac{\partial \boldsymbol{r}_\mathrm{i}}{\partial t} = \boldsymbol{v}_\mathrm{i} \\
\dfrac{\partial \boldsymbol{v}_\mathrm{i}}{\partial t} = \boldsymbol{F}_\mathrm{i}\left(\boldsymbol{r}_\mathrm{ij}, \boldsymbol{s}_\mathrm{i,j}\right) \\
\boxed{\dfrac{\partial \boldsymbol{s}_\mathrm{i}}{\partial t} = \boldsymbol{\omega}_\mathrm{i} \times \boldsymbol{s}_\mathrm{i}}
\end{cases}
$$

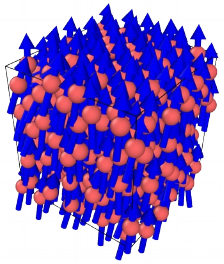

$$
\boldsymbol{H}_{sl} = \underbrace{\sum_{i=1}^{N} \frac{|\boldsymbol{p}_i|^2}{2m_i} + \sum_{i,j=1}^{N} V\left(r_{ij}\right)}_{\text{MD Hamiltonian}} \underbrace{- \sum_{i,j,i\neq j}^{N} J\left(r_{ij}\right) \boldsymbol{s}_i \cdot \boldsymbol{s}_j - \mu_B \mu_0 \sum_{i=0}^{N} g_i \boldsymbol{s}_i \cdot \boldsymbol{H}_{ext}}_{\text{Spin-lattice coupling}}
$$

Antropov, V. P., et al. (1996). Spin dynamics in magnets: Equation of motion and finite temperature effects. Phys. Rev. B, 54(2), 1019.

- Resolution of spin-waves, magnon modes.
- Adiabatic approximation: electronic dynamics frozen.
- Atomic spin: time average of the spin density over V atom.

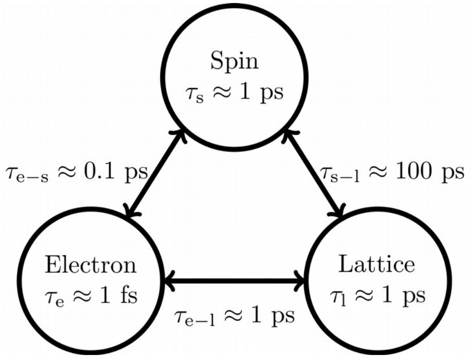

- Enables: magneto-elasticity, spin-lattice relaxation, magnon-phonon scattering, magneto-structural phase-transitions, ...

A computational model coupling micro-structure and magnetic properties

NVE and NVT ensembles

- Geometric integration algorithms enable NVE calculations.
- Langevin thermostat on the spins for NVT calculations.

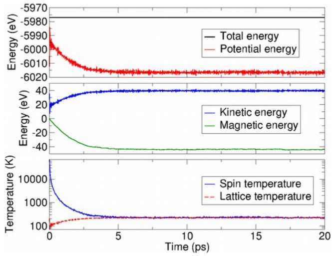

A computational model coupling micro-structure and magnetic properties

NVE and NVT ensembles

- Geometric integration algorithms enable NVE calculations.
- Langevin thermostat on the spins for NVT calculations.

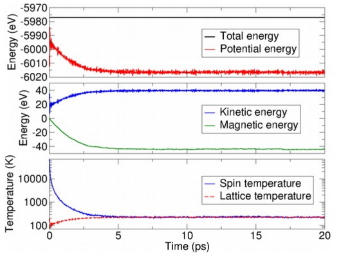

Three spin minimizers

- Damped dynamics with adaptive timestep, CG and LBFGS.
- Minimization on the energy, or on the total or per-atom torque.

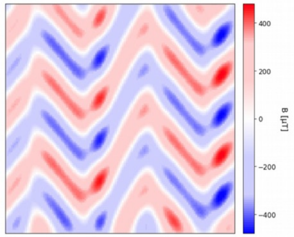

A computational model coupling micro-structure and magnetic properties

NVE and NVT ensembles

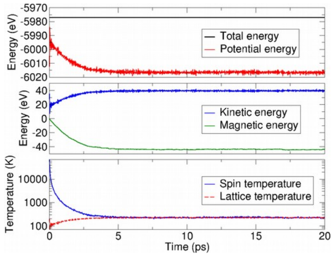

- Geometric integration algorithms enable NVE calculations.
- Langevin thermostat on the spins for NVT calculations.

Three spin minimizers

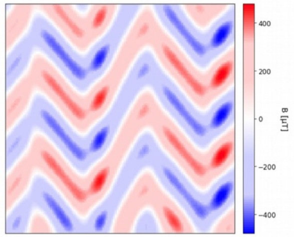

- Damped dynamics with adaptive timestep, CG and LBFGS.
- Minimization on the energy, or on the total or per-atom torque.

Eight different magnetic interactions

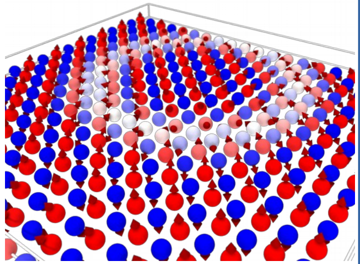

- Five pairs: exchange, DMI, Neel, Magneto-electric, dipolar.
- Three fixes: Zeeman, cubic and uniaxial anisotropies, and setforce.

A computational model coupling micro-structure and magnetic properties

NVE and NVT ensembles

- Geometric integration algorithms enable NVE calculations.
- Langevin thermostat on the spins for NVT calculations.

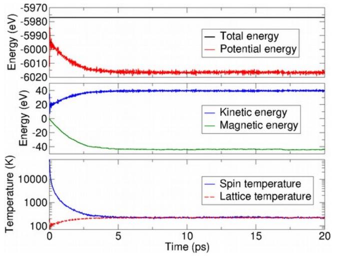

Three spin minimizers

- Damped dynamics with adaptive timestep, CG and LBFGS.
- Minimization on the energy, or on the total or per-atom torque.

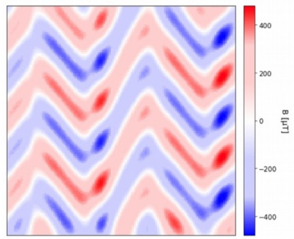

Eight different magnetic interactions

- Five pairs: exchange, DMI, Neel, Magneto-electric, dipolar.
- Three fixes: Zeeman, cubic and uniaxial anisotropies, and setforce.

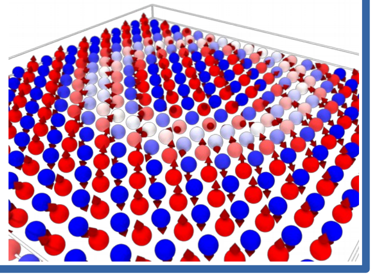

LAMMPS I/O for magnetic systems

- Output per-atom spin, per-atom and total mag energy, magnetic temperature, ...
- Read/restart from generated magnetic configutations.

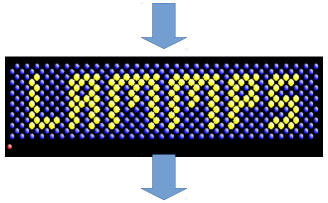

A computational model coupling micro-structure and magnetic properties

NVE and NVT ensembles

- Geometric integration algorithms enable NVE calculations.
- Langevin thermostat on the spins for NVT calculations.

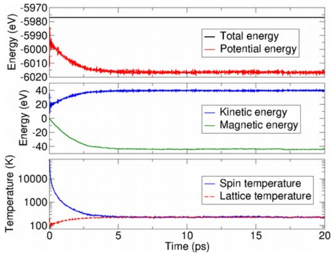

Three spin minimizers

- Damped dynamics with adaptive timestep, CG and LBFGS.
- Minimization on the energy, or on the total or per-atom torque.

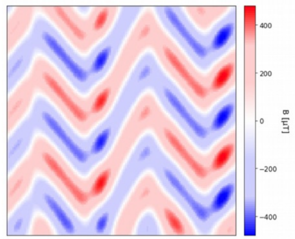

Eight different magnetic interactions

- Five pairs: exchange, DMI, Neel, Magneto-electric, dipolar.
- Three fixes: Zeeman, cubic and uniaxial anisotropies, and setforce.

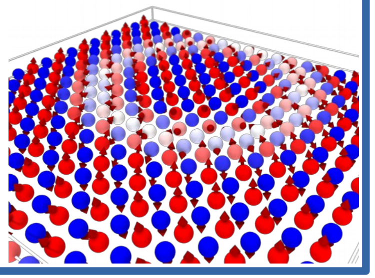

LAMMPS I/O for magnetic systems

- Output per-atom spin, per-atom and total mag energy, magnetic temperature, ...
- Read/restart from generated magnetic configutations.

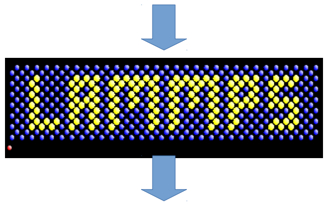

Geodesic NEB calculations

- Calculate energy barriers between magnetic configurations.
- Collaboration with Hannes Jonsson, Aleksei Ivanov and Pavel Bessarab.

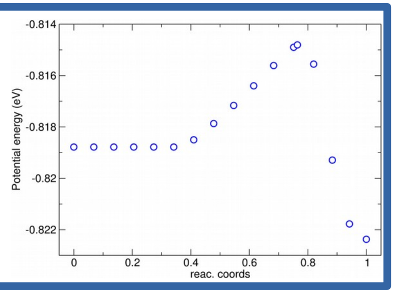

A computational model coupling micro-structure and magnetic properties

NVE and NVT ensembles

- Geometric integration algorithms enable NVE calculations.
- Langevin thermostat on the spins for NVT calculations.

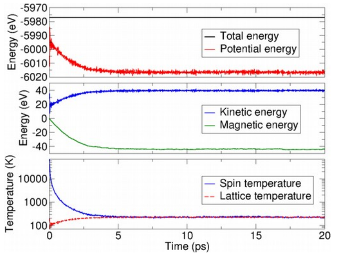

Three spin minimizers

- Damped dynamics with adaptive timestep, CG and LBFGS.
- Minimization on the energy, or on the total or per-atom torque.

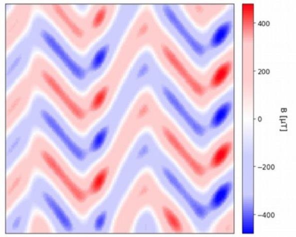

Eight different magnetic interactions

- Five pairs: exchange, DMI, Neel, Magneto-electric, dipolar.
- Three fixes: Zeeman, cubic and uniaxial anisotropies, and setforce.

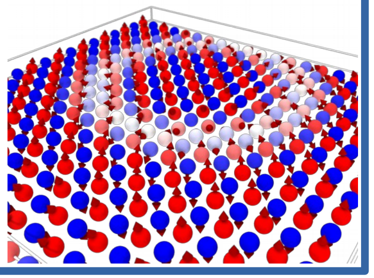

LAMMPS I/O for magnetic systems

- Output per-atom spin, per-atom and total mag energy, magnetic temperature, ...
- Read/restart from generated magnetic configutations.

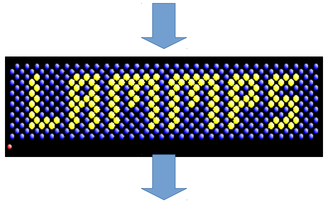

Geodesic NEB calculations

- Calculate energy barriers between magnetic configurations.
- Collaboration with Hannes Jonsson, Aleksei Ivanov and Pavel Bessarab.

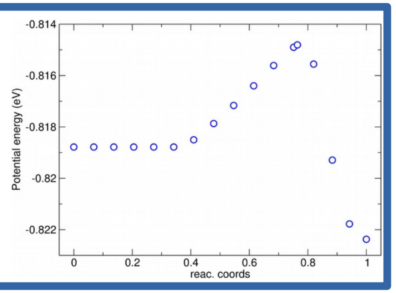

Long-range dipolar fields

- Ewald and P3M implemented to calculate long-range magnetic dipolar interactions.
- Nucleate and stabilize magnetic domains and domain-walls.

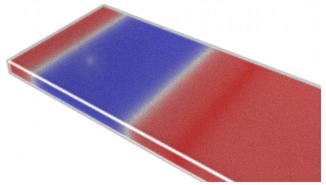

Chiral magnetic textures in multiferroics

Collaboration with M. Viret, J.-Y. Chauleau and T. Chirac at CEA

- Material: Bismuth ferrite $BiFeO_3$ (prototypical multiferroic, AF and ferroelectric at room temperature)
- Simulation of chiral magnetic textures at ferroelectric domain-walls.

Chiral magnetic textures in multiferroics

Collaboration with M. Viret, J.-Y. Chauleau and T. Chirac at CEA

- Material: Bismuth ferrite BiFeO3 (prototypical multiferroic, AF and ferroelectric at room temperature)
- Simulation of chiral magnetic textures at ferroelectric domain-walls.

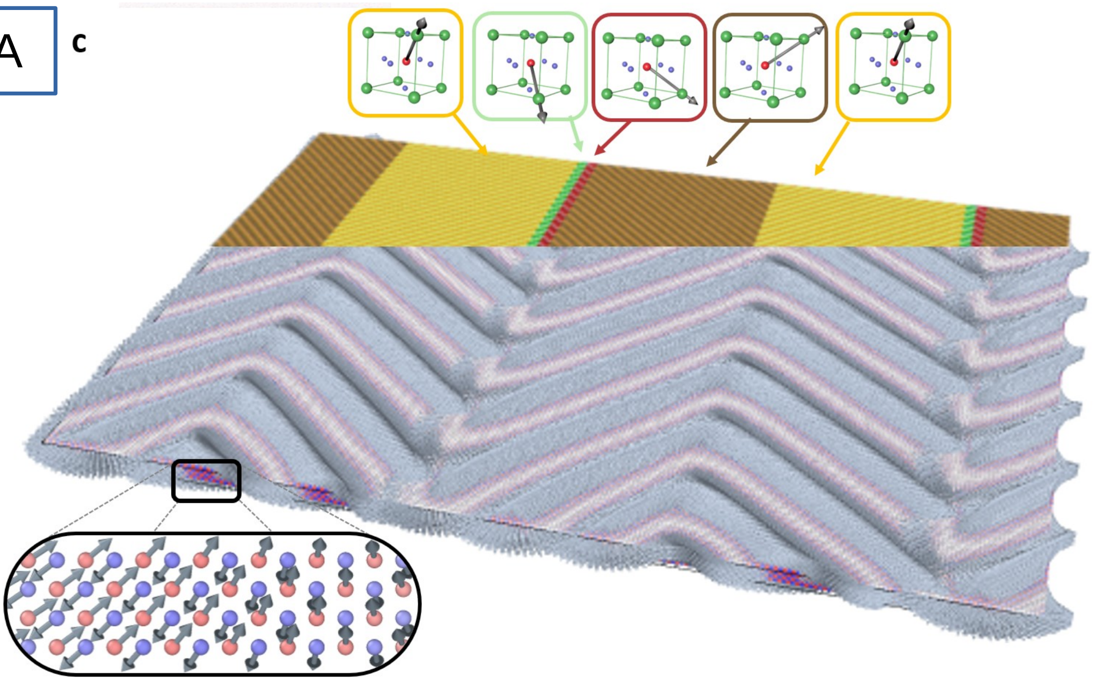

Simulation details

$$\mathcal{H}_{\mathrm{BFO}} = -\underbrace{\sum_{i,j,i\neq j}^{N} J_{ij}^{(1,2)}\, \boldsymbol{s}_i \cdot \boldsymbol{s}_j}_{\text{AF exchange}} + \underbrace{\sum_{i,j=1,i\neq j}^{N} \left(\boldsymbol{P}^{(A,B)} \times \boldsymbol{e}_{ij}\right) \cdot (\boldsymbol{s}_i \times \boldsymbol{s}_j)}_{\text{ME}} - \underbrace{\sum_{i=1}^{N} K_i\, (\boldsymbol{s}_i \cdot \boldsymbol{n}_i)^2}_{\text{Anisotropy}}$$

- Ferroelectric domains simulated by alternating the polarization vector **P** in the ME interaction.
- Simulation box of about 200k magnetic atoms
- Configuration relaxed in about 2 days on a 40 core-workstation

Chiral magnetic textures in multiferroics

Collaboration with M. Viret, J.-Y. Chauleau and T. Chirac at CEA

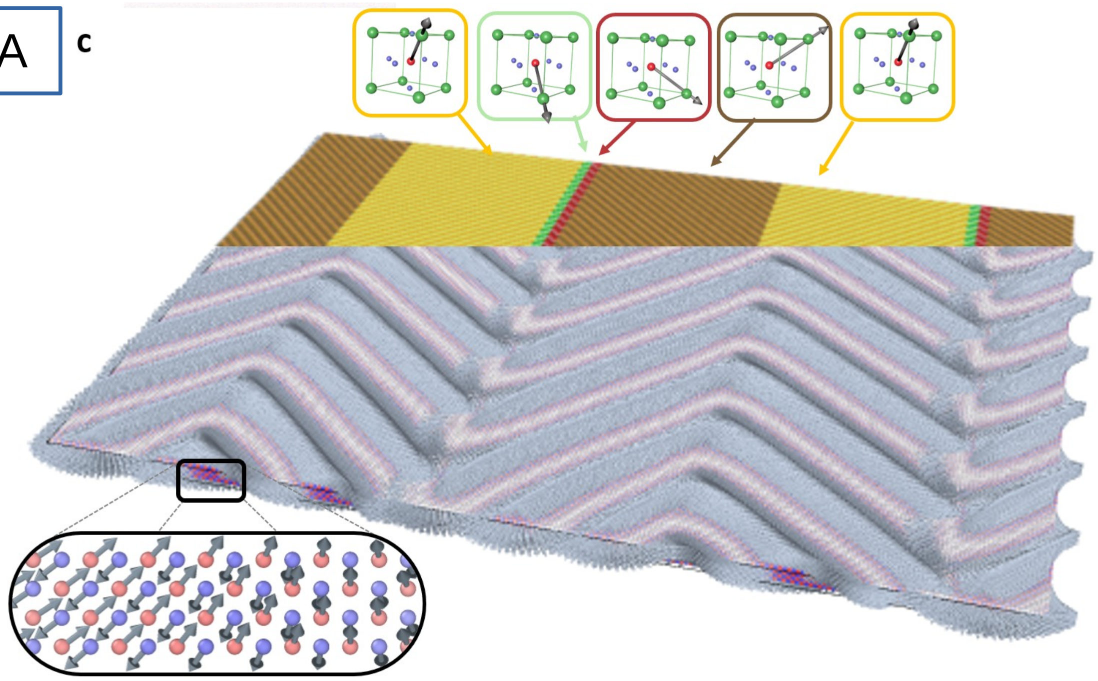

- Material: Bismuth ferrite $BiFeO_3$ (prototypical multiferroic, AF and ferroelectric at room temperature)
- Simulation of chiral magnetic textures at ferroelectric domain-walls.

Simulation details

$$\mathcal{H}_{\mathrm{BFO}} = -\underbrace{\sum_{i,j,i\neq j}^{N} J_{ij}^{(1,2)}\, \boldsymbol{s}_i \cdot \boldsymbol{s}_j}_{\text{AF exchange}} + \underbrace{\sum_{i,j=1,i\neq j}^{N} \left(\boldsymbol{P}^{(A,B)} \times \boldsymbol{e}_{ij}\right) \cdot \left(\boldsymbol{s}_i \times \boldsymbol{s}_j\right)}_{\text{ME}} - \underbrace{\sum_{i=1}^{N} K_i \left(\boldsymbol{s}_i \cdot \boldsymbol{n}_i\right)^2}_{\text{Anisotropy}}$$

- Ferroelectric domains simulated by alternating the polarization vector **P** in the ME interaction.
- Simulation box of about 200k magnetic atoms
- Configuration relaxed in about 2 days on a 40 core-workstation

- Results were compared with experimental measurements (performed by NV center). Very good agreement was recovered.

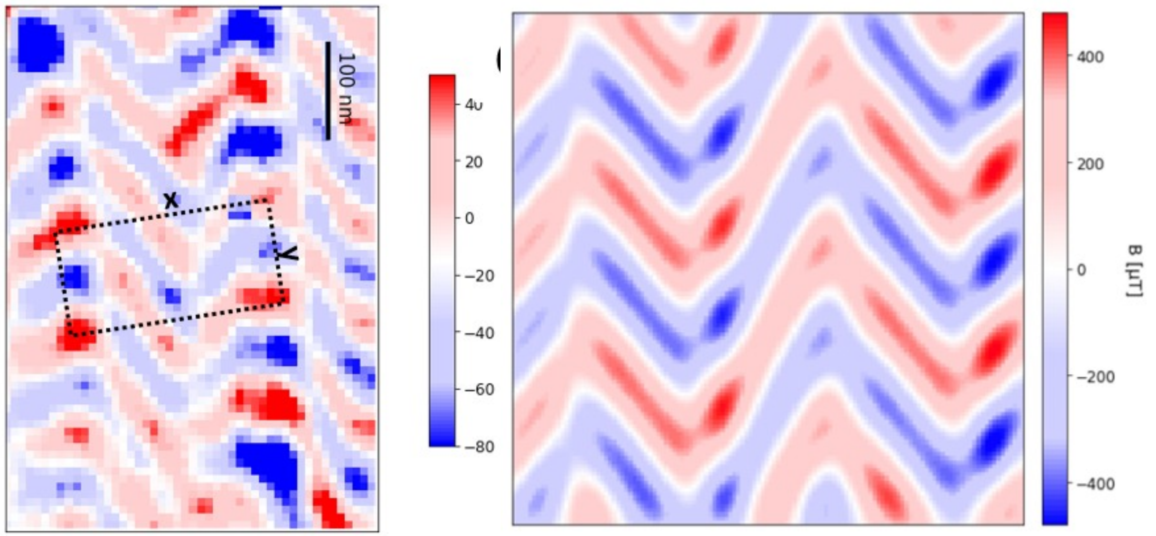

Thermal transport in magnetic materials

Collaboration with UCLA, YG Zhou, J. Murthy, T.S. Fisher.

- Abnormal behavior: drop of the lattice thermal conductivity at Tc.
- Development of a Green-Kubo equilibrium atomic and spin dynamics (GK-EASD) approach in LAMMPS.
- Development of better exchange models and statistics could greatly improve the accuracy.

Lattice thermal conductivity

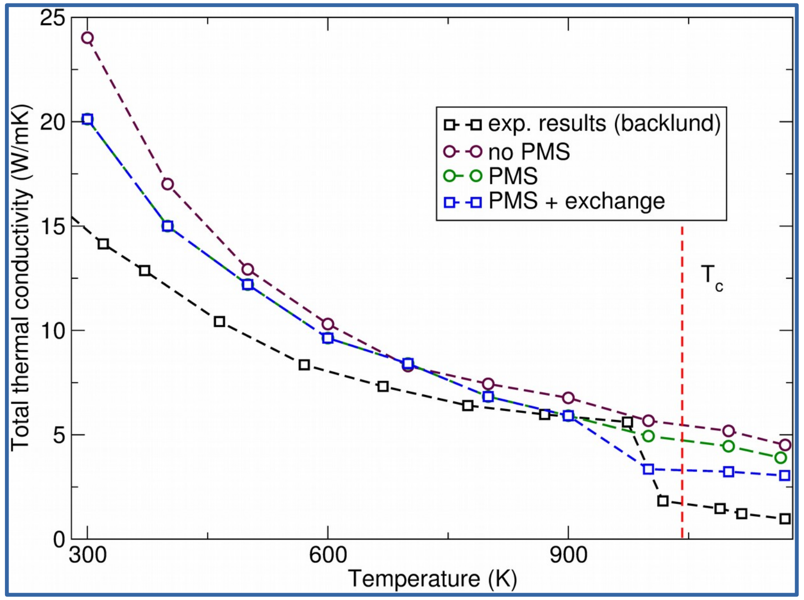

Bäcklund, N. G. (1961). . Journal of Phys. and Chem. of Solids, 20(1-2), 1-16.

Norm of total magnetization

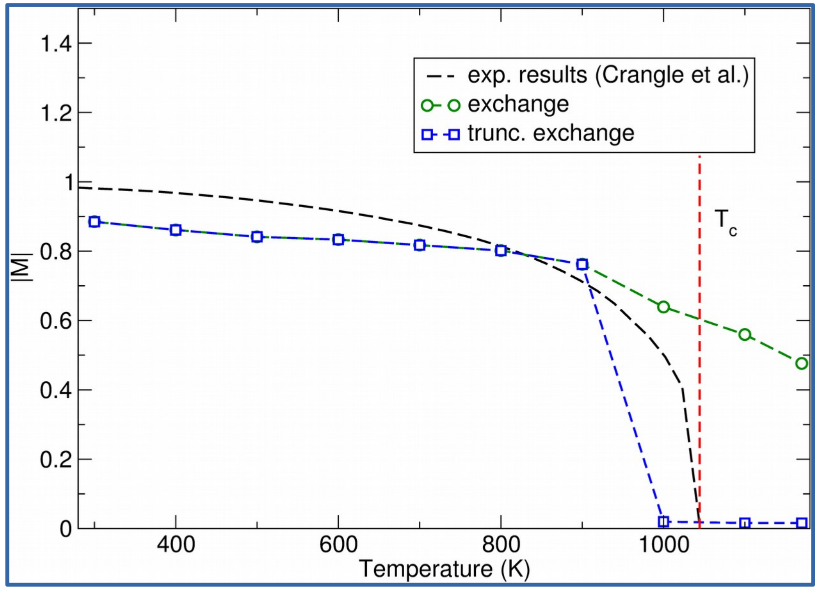

J. Crangle and GM Goodman, Proc. R. Soc. London, Ser. A 321, 477 (1971). Proc. R. Soc. London, Ser. A, 321, 477.

Magnetic dipole-dipole interaction

Long-range SD - MD

$$\begin{cases} \frac{\partial \boldsymbol{r}_{\mathrm{i}}}{\partial t} = \boldsymbol{v}_{\mathrm{i}} \\ \frac{\partial \boldsymbol{v}_{\mathrm{i}}}{\partial t} = \boldsymbol{F}_{\mathrm{i}}\left(\boldsymbol{r}_{\mathrm{ij}}, \boldsymbol{s}_{\mathrm{i,j}}\right) \\ \frac{\partial \boldsymbol{s}_{\mathrm{i}}}{\partial t} = \boldsymbol{\omega}_{\mathrm{i}} \times \boldsymbol{s}_{\mathrm{i}} \end{cases}$$

$$\mathcal{H}_{\text{long}} = -\frac{\mu_0 \left(\mu_B\right)^2}{4\pi} \sum_{i,j,i\neq j}^{N} \frac{g_i g_j}{r_{ij}^3} \left(3\left(\boldsymbol{e}_{ij}\cdot\boldsymbol{s}_i\right)\left(\boldsymbol{e}_{ij}\cdot\boldsymbol{s}_j\right) - \boldsymbol{s}_i\cdot\boldsymbol{s}_j\right)$$

$$\boldsymbol{F}_i = \frac{\mu_0(\mu_B)^2}{4\pi} \sum_j \frac{g_i g_j}{r_{ij}^4} \left[\left((\boldsymbol{s}_i\cdot\boldsymbol{s}_j) - 5(\boldsymbol{e}_{ij}\cdot\boldsymbol{s}_i)(\boldsymbol{e}_{ij}\cdot\boldsymbol{s}_j)\right)\boldsymbol{e}_{ij} + \left((\boldsymbol{e}_{ij}\cdot\boldsymbol{s}_i)\boldsymbol{s}_j + (\boldsymbol{e}_{ij}\cdot\boldsymbol{s}_j)\boldsymbol{s}_i\right)\right]$$

$$\boldsymbol{\omega}_i = \frac{\mu_0(\mu_B)^2}{4\pi\hbar} \sum_j \frac{g_i g_j}{r_{ij}^3} \left(3\left(\boldsymbol{e}_{ij}\cdot\boldsymbol{s}_j\right)\boldsymbol{e}_{ij} - \boldsymbol{s}_j\right)$$

Magnetic dipole-dipole interaction

Long-range SD - MD

$$\left\{\begin{array}{lcl} \frac{\partial \boldsymbol{r}_\mathrm{i}}{\partial t} & = & \boldsymbol{v}_\mathrm{i} \\ \frac{\partial \boldsymbol{v}_\mathrm{i}}{\partial t} & = & \boldsymbol{F}_\mathrm{i}\left(\boldsymbol{r}_\mathrm{ij}, \boldsymbol{s}_\mathrm{i,j}\right) \\ \frac{\partial \boldsymbol{s}_\mathrm{i}}{\partial t} & = & \boldsymbol{\omega}_\mathrm{i} \times \boldsymbol{s}_\mathrm{i} \end{array}\right.$$

$$\left\{\begin{array}{l} \mathcal{H}_{\mathrm{long}} = -\frac{\mu_0 \left(\mu_B\right)^2}{4\pi} \sum_{i,j,i\neq j}^{N} \frac{g_i g_j}{r_{ij}^3} \left(3\left(\boldsymbol{e}_{ij}\cdot\boldsymbol{s}_i\right)\left(\boldsymbol{e}_{ij}\cdot\boldsymbol{s}_j\right) - \boldsymbol{s}_i\cdot\boldsymbol{s}_j\right) \\ \boldsymbol{F}_i = \frac{\mu_0(\mu_B)^2}{4\pi} \sum_j \frac{g_i g_j}{r_{ij}^4} \left[\left((\boldsymbol{s}_i\cdot\boldsymbol{s}_j) - 5(\boldsymbol{e}_{ij}\cdot\boldsymbol{s}_i)(\boldsymbol{e}_{ij}\cdot\boldsymbol{s}_j)\right)\boldsymbol{e}_{ij} + \left((\boldsymbol{e}_{ij}\cdot\boldsymbol{s}_i)\boldsymbol{s}_j + (\boldsymbol{e}_{ij}\cdot\boldsymbol{s}_j)\boldsymbol{s}_i\right)\right] \\ \boldsymbol{\omega}_i = \frac{\mu_0(\mu_B)^2}{4\pi\hbar} \sum_j \frac{g_i g_j}{r_{ij}^3} \left(3\left(\boldsymbol{e}_{ij}\cdot\boldsymbol{s}_j\right)\boldsymbol{e}_{ij} - \boldsymbol{s}_j\right) \end{array}\right.$$

- Two methods implemented: Ewald and P3M (P3M also implemented for electric dipoles).

Magnetic dipole-dipole interactions

Long-range SD - MD

$$
\begin{cases}
\dfrac{\partial \boldsymbol{r}_{\mathrm{i}}}{\partial t} = \boldsymbol{v}_{\mathrm{i}} \\
\dfrac{\partial \boldsymbol{v}_{\mathrm{i}}}{\partial t} = \boldsymbol{F}_{\mathrm{i}}\left(\boldsymbol{r}_{\mathrm{ij}}, \boldsymbol{s}_{\mathrm{i,j}}\right) \\
\dfrac{\partial \boldsymbol{s}_{\mathrm{i}}}{\partial t} = \boldsymbol{\omega}_{\mathrm{i}} \times \boldsymbol{s}_{\mathrm{i}}
\end{cases}
$$

$$
\begin{cases}
\mathcal{H}_{\mathrm{long}} = -\dfrac{\mu_0 \left(\mu_B\right)^2}{4\pi} \displaystyle\sum_{i,j,i\neq j}^{N} \dfrac{g_i g_j}{r_{ij}^3} \left(3\left(\boldsymbol{e}_{ij}\cdot\boldsymbol{s}_i\right)\left(\boldsymbol{e}_{ij}\cdot\boldsymbol{s}_j\right) - \boldsymbol{s}_i\cdot\boldsymbol{s}_j\right) \\
\boldsymbol{F}_i = \dfrac{\mu_0 (\mu_B)^2}{4\pi} \displaystyle\sum_j \dfrac{g_i g_j}{r_{ij}^4} \left[\left((\boldsymbol{s}_i\cdot\boldsymbol{s}_j) - 5(\boldsymbol{e}_{ij}\cdot\boldsymbol{s}_i)(\boldsymbol{e}_{ij}\cdot\boldsymbol{s}_j)\right)\boldsymbol{e}_{ij} + \left((\boldsymbol{e}_{ij}\cdot\boldsymbol{s}_i)\boldsymbol{s}_j + (\boldsymbol{e}_{ij}\cdot\boldsymbol{s}_j)\boldsymbol{s}_i\right)\right] \\
\boldsymbol{\omega}_i = \dfrac{\mu_0 (\mu_B)^2}{4\pi\hbar} \displaystyle\sum_j \dfrac{g_i g_j}{r_{ij}^3} \left(3\left(\boldsymbol{e}_{ij}\cdot\boldsymbol{s}_j\right)\boldsymbol{e}_{ij} - \boldsymbol{s}_j\right)
\end{cases}
$$

- Two methods implemented: Ewald and P3M (P3M also implemented for electric dipoles).

Scaling results

- From 1 to 32 Broadwell nodes, with 36 processes per node (1024 processes for the last point).
- Spin-lattice Ewald has the same scaling as Ewald/disp (reference in LAMMPS).
- Spin-lattice PPPM faster and much better scaling.

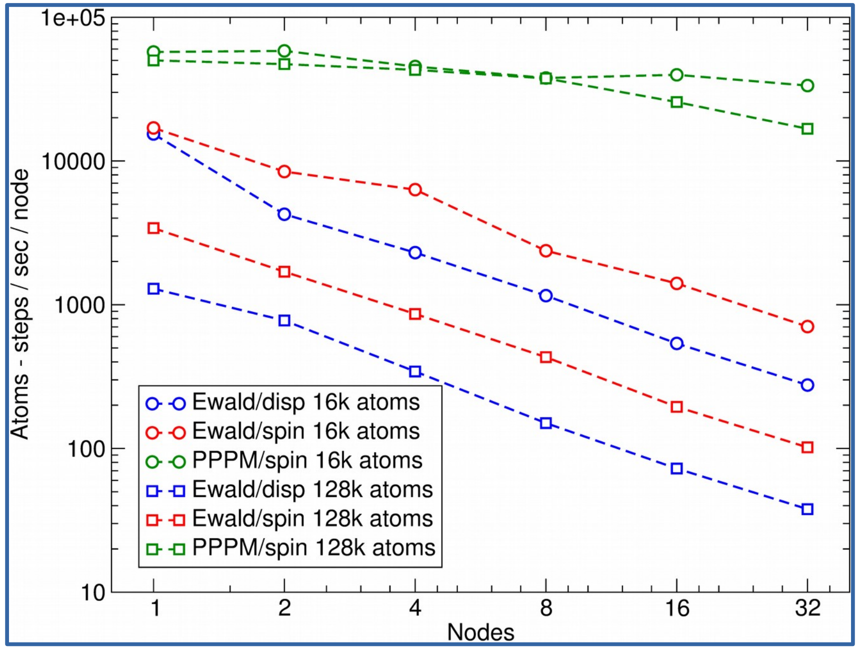

Magnetic dipole-dipole interaction

Long-range SD - MD

$$\begin{cases} \frac{\partial \boldsymbol{r}_{\mathrm{i}}}{\partial t} = \boldsymbol{v}_{\mathrm{i}} \\ \frac{\partial \boldsymbol{v}_{\mathrm{i}}}{\partial t} = \boldsymbol{F}_{\mathrm{i}}\left(\boldsymbol{r}_{\mathrm{ij}}, \boldsymbol{s}_{\mathrm{i,j}}\right) \\ \frac{\partial \boldsymbol{s}_{\mathrm{i}}}{\partial t} = \boldsymbol{\omega}_{\mathrm{i}} \times \boldsymbol{s}_{\mathrm{i}} \end{cases}$$

$$\begin{cases} \mathcal{H}_{\mathrm{long}} = -\frac{\mu_0 (\mu_B)^2}{4\pi} \sum_{i,j,i\neq j}^{N} \frac{g_i g_j}{r_{ij}^3} \left(3 (\boldsymbol{e}_{ij} \cdot \boldsymbol{s}_i)(\boldsymbol{e}_{ij} \cdot \boldsymbol{s}_j) - \boldsymbol{s}_i \cdot \boldsymbol{s}_j\right) \\ \boldsymbol{F}_i = \frac{\mu_0 (\mu_B)^2}{4\pi} \sum_j \frac{g_i g_j}{r_{ij}^4} \left[\left((\boldsymbol{s}_i \cdot \boldsymbol{s}_j) - 5 (\boldsymbol{e}_{ij} \cdot \boldsymbol{s}_i)(\boldsymbol{e}_{ij} \cdot \boldsymbol{s}_j) \right) \boldsymbol{e}_{ij} + \left((\boldsymbol{e}_{ij} \cdot \boldsymbol{s}_i) \boldsymbol{s}_j + (\boldsymbol{e}_{ij} \cdot \boldsymbol{s}_j) \boldsymbol{s}_i \right) \right] \\ \boldsymbol{\omega}_i = \frac{\mu_0 (\mu_B)^2}{4\pi\hbar} \sum_j \frac{g_i g_j}{r_{ij}^3} \left(3 (\boldsymbol{e}_{ij} \cdot \boldsymbol{s}_j) \boldsymbol{e}_{ij} - \boldsymbol{s}_j \right) \end{cases}$$

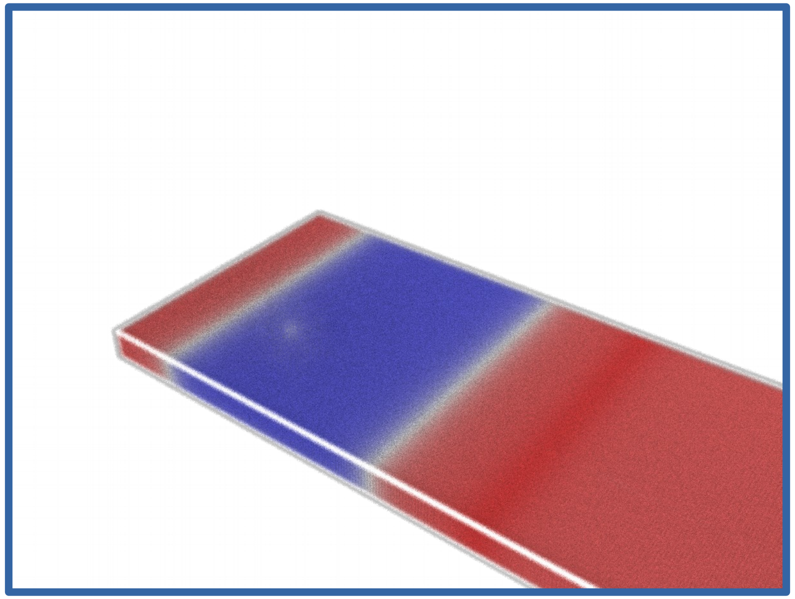

Domain-wall nucleation

- Allows the simulation of nucleation and motion of magnetic domains and domain-walls.
- Goal: bridging ab initio and continuum scale magnetic calculations.

Conclusions

- SPIN package available in LAMMPS.
- Enables massively parallel spin-lattice dynamics to be performed with LAMMPS.
- The model adds new physics into LAMMPS, is accurate, scales very well with the number of processes, and only 5 times slower than usual MD – EAM calculations.
- Accounts for a lot of magnetic interactions. Models for the spin-orbit coupling are currrently being developed.
- Open to collaborations, feel free to contact us (jtranch@sandia.gov).

- Thanks to the LAMMPS group at Sandia: Aidan, Steve, Mitch, Stan, Mary-Alice.
- And at Temple U.: Axel and Richard.

http://lammps.sandia.gov/

https://github.com/lammps/lammps

- Thanks to my co-workers at UCLA: YG Zhou, Pr. Fisher, Pr. Murthy.
- And at CEA: Pascal Thibaudeau, Michel Viret, Jean-Yves Chauleau, Theophile Chirac.

Thank you for hosting me and for you attention.

Potential improvements, ongoing developments

Pressure and temperature effects

- Need to account for longitudinal spin fluctuations.

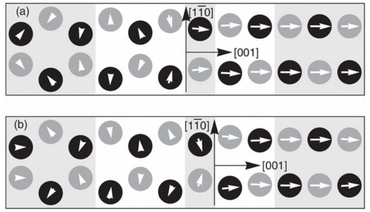

- Example: magneto-structural phase transitions (alpha → epsilon in iron)

Surh, M. P., et al. (2016). Magnetostructural transition kinetics in shocked iron. Phys.Rev.Lett., 117(8), 085701.

Electronic degrees of freedom in MD

- TD-DFT parametrization of a 3-temperature model:.

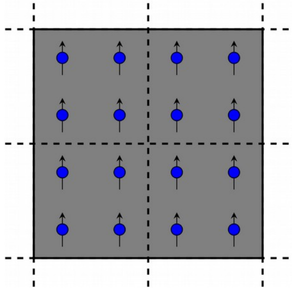

- Longitudinal spin fluctuations parametrized on Te.

Kinetic of magnetism

- Visit of Hannes Jonsson's group in January.

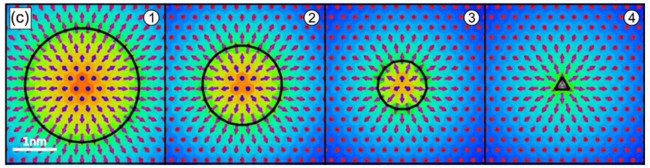

- Implementation of a magnetic NEB, and begin development of a spin-lattice version.

Bessarab, P. F., et al. (2018). Lifetime of racetrack skyrmions. Scientific reports, 8(1), 3433.

Magnetostriction

- Models for effects of the SOC

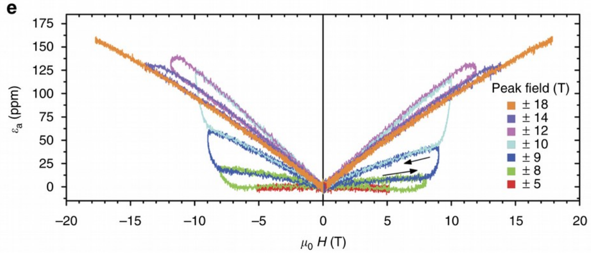

- Example: cobalt, gadolinium, uranium dioxide

Jaime, M., et al. (2017). Nature communications, 8(1), 99.

Phase-transition and defects in metals

- Irradiation-based defects in bcc iron:

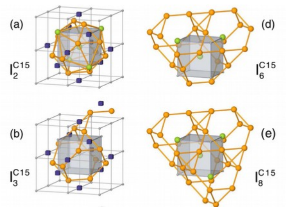

Vacancies.

Interstitial sites.

- Need Ab intio exchange parameters.

Marinica, M. C., et al. (2012). Physical Review Letters, 108(2), 025501.

Simulation of multiferroics

- Example: bismuth oxide

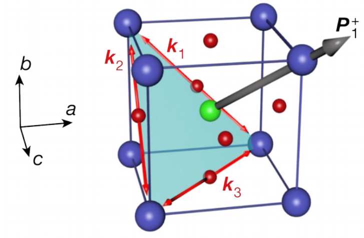

Bismuth
Oxygen
Iron

- Magnetic (AF) and ferroelectric orders.

Juraschek, D. M., et al. (2017). Dynamical multiferroicity. Physical Review Materials, 1(1), 014401.

Accounting for the spin-lattice interactions

- The current version accounts for six magnetic interactions:

Exchange interaction:

$$\boldsymbol{H}_{exchange} = -\sum_{i,j,i\neq j}^{N} J\left(r_{ij}\right) \vec{s}_i \cdot \vec{s}_j$$

- Simulation of ferromagnetism, antiferromagnetism, ferrimagnetism, ...

Uniaxial anisotropy:

$$\boldsymbol{H}_{an} = -\sum_{i=1}^{N} K_{an}(\boldsymbol{r}_i) \left(\boldsymbol{s}_i \cdot \boldsymbol{n}_i\right)^2$$

- Simulation of magnetocrystalline anisotry or shape anisotropy.
- ✖ Poor lattice dependence.

Dzyaloshinskii-Moriya:

$$\boldsymbol{H}_{dm} = \sum_{i,j=1,i\neq j}^{N} \vec{D}\left(r_{ij}\right) \cdot \left(\vec{s}_i \times \vec{s}_j\right),$$

- Simulation of an effect of the spin-orbit coupling
- Very trendy (chiral magnetism, skyrmions...)

Zeeman interaction:

$$\boldsymbol{H}_{Zeeman} = -\mu_B \mu_0 \sum_{i=0}^{N} g_i\, \boldsymbol{s}_i \cdot \boldsymbol{H}_{ext}$$

- Interaction with an external magnetic field (constant or time dependent).

Magneto-electric interaction:

$$\boldsymbol{H}_{me} = -\sum_{i,j,i\neq j}^{N} \left(\vec{E} \times \vec{e}_{ij}\right) \cdot \left(\vec{s}_i \times \vec{s}_j\right),$$

- Interaction between spins and electric dipoles.
- Simulation of multiferroic materials.

Katsura, H.,et al. (2005). Spin current and magnetoelectric effect in noncollinear magnets. Phys. Rev. Lett., 95(5), 057205.

Néel pair anisotropy:

$$\boldsymbol{H}_{N\acute{e}el} = -\sum_{i,j=1,i\neq j}^{N} g_1(r_{ij}) \left((\boldsymbol{e}_{ij} \cdot \boldsymbol{s}_i)(\boldsymbol{e}_{ij} \cdot \boldsymbol{s}_j) - \frac{\boldsymbol{s}_i \cdot \boldsymbol{s}_j}{3} \right)$$

- Other way to account for effects of the spin-orbit coupling.
- Simulation of magnetocrystalline anisotropy and magneto-elasticity.

Bruno, P. (1988). Magnetic surface anisotropy of cobalt and surface roughness effects within Neel's model. J. Phys. F: Metal Physics, 18(6), 1291.